Journal of Sound and Vibration (1997) **201**(3), 305–321

ACOUSTIC TWO-DIMENSIONAL RADIATION AND SCATTERING FROM CYLINDERS USING SOURCE DENSITY, SVD AND FOURIER METHODS

P. R. Stepanishen

Department of Ocean Engineering, University of Rhode Island, Kingston, RI 02881-0814, *U.S.A.*

(*Received* 26 *April* 1996, *and in final form* 20 *August* 1996)

Acoustic two-dimensional harmonic radiation and rigid body scattering from cylinders of arbitrary shape with a plane of symmetry are addressed using an internal line monopole and dipole source distribution along the plane of symmetry. A previously developed least mean square error method is used to solve the Neumann boundary value problem. In contrast to the earlier method, Singular Value Decomposition (SVD) methods are presented to determine the line source harmonic multipole distributions from the specified normal velocity at the cylindrical surface and pressures are simply expressed here as line integrals of the source distributions which in the far field reduce to Fourier transform relationships. Several special examples are presented to illustrate the general spatial characteristics of the source strength distributions for cylinders with widely varying aspect ratios. Exact source strength distributions for circular cylinders are developed using the Fourier transform relationships. The resulting source strength distributions involve spatial derivatives of Dirac delta functions and thus have a vanishingly small region of support about the center of the cylinder. In contrast, for cylinders with large aspect ratios the spatial characteristics of the source strength distributions are more closely matched to the normal velocity distribution.

1. INTRODUCTION

Acoustic two-dimensional harmonic radiation and rigid body scattering may be formulated as classical boundary value problems in physics. Such problems require the solution of the reduced scalar wave equation subject to specified boundary conditions on the surface or contour of interest. Similar boundary value problems occur in a wide range of hydrodynamic, elastic and electromagnetic field problems. There are thus a multitude of well known and established analytical methods [1, 2] which have been developed to address such problems. More recent developments and techniques are included in the lecture notes of Crighton *et al*. [3].

Bowman *et al*. [4] have compiled a comprehensive summary of classical methods and numerical results for electromagnetic and acoustic scattering by bodies of various shapes for which the wave equation is separable. Extensive numerical results for both two- and three-dimensional harmonic problems are presented for line source, point source and plane wave excitations. In particular, numerical results are presented for various two-dimensional scattering problems involving infinite strips, circular and elliptical cylinders.

Two-dimensional acoustic harmonic radiation and scattering from rigid cylinders is still a research topic of interest. As a result of the availability of computers, integral equation

0022–460X/97/130305 + 17 $25.00/0/sv960726

methods [5–7] have become the method of present choice for addressing the general acoustic harmonic radiation and scattering problem at low and mid-frequencies for arbitrary geometries. Such methods have well recognized shortcomings; e.g., at high frequencies. Alternative methods of solution thus continue to be developed.

In the present paper acoustic two-dimensional harmonic radiation and rigid body scattering problems from cylinders of arbitrary shape with a plane of symmetry are addressed. A previously developed Least Mean Square (LMS) error method [8–10] is used to solve the Neumann boundary value problem via the use of an internal line monopole and dipole source distribution along the plane of symmetry. Singular Value Decomposition (SVD) methods are presented to determine the line source harmonic multi-pole distributions from the specified normal velocity at the cylindrical surface. Also, in contrast to the earlier method in which the surface pressure was first evaluated from the source distributions and then the Helmholtz integral was used to evaluate the field, pressures are simply obtained here from line integrals of the source distributions which in the far field reduce to Fourier transform relationships.

In the earlier papers on the subject, numerical studies of the basic LMS method to address acoustic radiation and scattering problems were presented. Numerical results were presented to illustrate the characteristics of the source distributions and the associated pressure fields for cylindrical and elliptical cylinders. Analytical methods are employed here to determine closed form solutions for the source distributions for selected geometries. Several special examples are presented to illustrate the general spatial characteristics of the source strength distributions for cylinders with widely varying aspect ratios. Exact source strength distributions for circular cylinders are developed using the Fourier transform relationships. The resulting source strength distributions involve spatial derivatives of Dirac delta functions and thus have a vanishingly small region of support about the center of the cylinder. In contrast, for cylinders with large aspect ratios the spatial characteristics of the source strength distributions are shown to be more closely matched to the normal velocity distribution.

2. THEORY

Consider a smooth cylinder which has a plane of symmetry and is in contact with an external ideal fluid as shown in Figure 1. Since the acoustic two-dimensional harmonic radiation and scattering problem is of interest here, the incident harmonic pressure field and/or the harmonic normal velocity on the surface of the cylinder are specified. The total harmonic pressure field in the external fluid is to be determined.

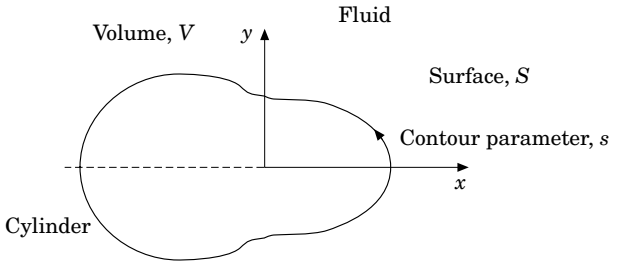

Figure 1. A cylinder with plane of symmetry.

In order to address the acoustic radiation/scattering problem of interest it is convenient to first note that the total pressure field can be expressed as

$$p_t(\mathbf{x}) = p_i(\mathbf{x}) + p(\mathbf{x}), \tag{1}$$

where the total pressure field $p_t(\mathbf{x})$ is decomposed into the incident harmonic pressure field $p_i(\mathbf{x})$ and the pressure field $p(\mathbf{x})$ which accounts for the radiation due to the specified normal velocity and/or the rigid cylinder scattering. This latter field can be posed as the solution of the following Neumann boundary value problem:

$$\nabla^2 p(\mathbf{x}) + k^2 p(\mathbf{x}) = 0, \qquad \mathbf{x} \in V, \tag{2a}$$

$$\frac{\partial p(\mathbf{x})}{\partial n} = -\frac{\partial p_i(\mathbf{x})}{\partial n} - \mathrm{j}k\rho_0 c_0 v_r(\mathbf{x}), \qquad \mathbf{x} \in S, \tag{2b}$$

$$\lim_{r \to \infty} r^{1/2}[\partial p/\partial r + \mathrm{j}kp] = 0, \tag{2c}$$

where k is the acoustic wavenumber, n denotes the exterior normal on the surface S, i.e., into the fluid volume V, and ρ_0 and c_0 are the density and acoustic wave speed of the fluid. In equation (2b) the incident pressure field and the normal velocity of the surface $v_r(\mathbf{x})$ for $\mathbf{x} \in S$ are specified functions. Equation (2c) is the Sommerfeld radiation condition which is required to ensure uniqueness of the solution [1–3].

In light of equations (1) and (2) it is obvious that if $p_i(\mathbf{x}) = 0$ for all $\mathbf{x} \in V$, then $p(\mathbf{x})$ is the solution of the radiation problem; however, if $v_r(\mathbf{x}) = 0$ for $\mathbf{x} \in S$, then $p(\mathbf{x})$ is the solution of the rigid body scattering problem. The total pressure field is thus considered here to be the superposition of the two fields. Interactions between the fields are neglected due to small amplitude assumptions; e.g., the interaction of the incident field with the moving boundary is neglected.

It is apparent from equations (1) and (2) that the acoustic radiation/scattered pressure field has been expressed as the solution of a Neumann boundary value problem where the normal velocity on the surface S is a specified function of position, i.e.,

$$v(s) = -v_i(\mathbf{x}_s) + v_r(\mathbf{x}_s), \tag{3}$$

where $v_i(\mathbf{x}_s)$ is the normal velocity of the incident wave field, $v_r(\mathbf{x}_s)$ is the specified normal velocity for the radiation problem and $\mathbf{x}_s$ is a position vector to a point on S, where s is a contour parameter on the cylinder with $0 < s < |s_{max}|$ as indicated in Figure 1. It is thus apparent that for either the acoustic radiation or scattering problem of present interest, $v(s)$ is a prescribed function on the surface S.

In general, the normal velocity $v(s)$ can be decomposed into symmetric and antisymmetric components as

$$v(s) = v^e(s) + v^o(s), \tag{4a}$$

where the symmetric component is

$$v^e(s) = \tfrac{1}{2}[v(s) + v(-s)] \tag{4b}$$

and the antisymmetric component is

$$v^o(s) = \tfrac{1}{2}[v(s) - v(-s)]. \tag{4c}$$

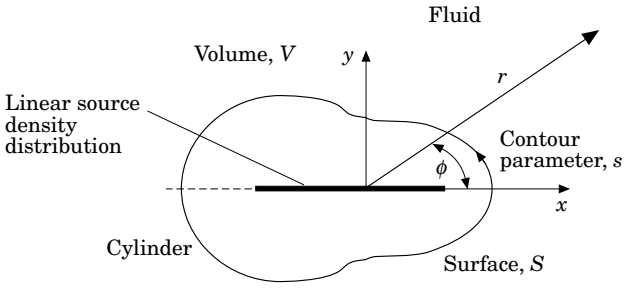

Figure 2. The linear source density distribution and geometry.

The pressure field $p(\mathbf{x})$ can then also be decomposed into symmetric and antisymmetric fields, i.e.,

$$p(\mathbf{x}) = p^e(\mathbf{x}) + p^o(\mathbf{x}), \tag{5}$$

where it is clearly apparent that $p^e(\mathbf{x})$ is determined by $v^e(s)$ and $p^o(\mathbf{x})$ is determined by $v^o(s)$.

Internal line source distributions along the plane of symmetry are now used here to determine the pressure field $p(\mathbf{x})$ in the external fluid. A detailed development of the method was presented in earlier papers [8, 9]; hence, a summary of the approach is presented here. To determine $p^e(\mathbf{x})$ ($p^o(\mathbf{x})$), linear distributions of monopole (dipole) line sources along the plane of symmetry of the surface are used to match the associated normal velocity component $v^e(s)$ ($v^o(s)$) indicated in equation (4). The resultant internal linear monopole and dipole source distributions, which are illustrated in Figure 2, automatically ensure the correct symmetry of the resultant pressure fields.

Consider first a linear distribution of unknown internal monopole line sources along the axis of symmetry of the surface. The associated pressure field in the fluid external to the cylinder can be expressed as the following line integral along the axis of symmetry of the surface:

$$p_m(\mathbf{x}) = \mathrm{j}k\rho_0 c_0 \int [g(\mathbf{x}, \mathbf{x}_0)]_{y_0=0} \sigma_m(x_0)\, \mathrm{d}x_0 \tag{6a}$$

where $\sigma_m(x)$ is the unknown monopole source density (source strength per unit length) at $y = 0$ and $g(\mathbf{x}, \mathbf{x}_0)$ is the two-dimensional free space Green function, i.e.,

$$g(\mathbf{x}, \mathbf{x}_0) = -(\mathrm{j}/4)\mathrm{H}_0(k\sqrt{(x - x_0)^2 + (y - y_0)^2}), \tag{6b}$$

where $\mathrm{H}_0()$ is the zeroth Hankel function of the second kind. On the surface S the pressure can then be expressed as

$$p_m(\mathbf{x}_s) = \mathrm{j}k\rho_0 c_0 \int [g(\mathbf{x}_s, \mathbf{x}_0)]_{y_0=0} \sigma_m(x_0)\, \mathrm{d}x_0 \tag{7a}$$

where $\mathbf{x}_s$ denotes a position vector to a point specified by s along the contour. It then follows from the linearized momentum equation that the associated normal velocity at the surface can be expressed as

$$v_m(s) = \int -\hat{\mathbf{n}} \cdot \nabla_s [g(\mathbf{x}_s, \mathbf{x}_0)]_{y_0=0} \sigma_m(x_0)\, \mathrm{d}x_0. \tag{7b}$$

Now consider a linear distribution of unknown internal dipole line sources along the axis of symmetry of the surface. The pressure field in the fluid external to the cylinder can be expressed as the following line integral along the axis of symmetry of the surface:

$$p_d(\mathbf{x}) = \int \left[\frac{\partial g(\mathbf{x}, \mathbf{x}_0)}{\partial y_0} \right]_{y_0 = 0} \sigma_d(x_0)\, \mathrm{d}x_0. \tag{8}$$

Here $\sigma_d(x)$ is an unknown dipole source density (dipole strength per unit length) at $y = 0$. The associated surface pressure field can then be expressed as the following line integral along the axis of symmetry of the surface,

$$p_d(\mathbf{x}_s) = \int \left[\frac{\partial g(\mathbf{x}_s, \mathbf{x}_0)}{\partial y_0} \right]_{y_0 = 0} \sigma_d(x_0)\, \mathrm{d}x_0 \tag{9a}$$

and the associated normal velocity on the surface can then be expressed as

$$v_d(s) = -\int \frac{\hat{\mathbf{n}}}{\mathrm{j}k\, \rho_0\, c_0} \cdot \nabla_s \left[\frac{\partial g(\mathbf{x}_s, \mathbf{x}_0)}{\partial y_0} \right]_{y_0 = 0} \sigma_d(x_0)\, \mathrm{d}x_0. \tag{9b}$$

An LMS or least mean square error criteria is now used to determine the unknown source strengths of the internal monopole and dipole source distributions [9]. More specifically, functionals J_e and J_o are introduced as follows to measure the error between the specified symmetric and antisymmetric component of the normal surface velocity $v(s)$ and that due to the appropriate internal source density distribution:

$$J_e = \int |v^e(s) - v_m(s)|^2\, \mathrm{d}s \qquad \text{and} \qquad J_0 = \int |v^o(s) - v_d(s)|^2\, \mathrm{d}s. \tag{10a, b}$$

The general procedure to minimize each of the functionals J_e and J_0 is identical. For both cases, the minimization procedure requires the solution of an integral equation,

$$\hat{v}(s) = \int_y k(s|x)\sigma(x)\, \mathrm{d}x \tag{11}$$

where $\hat{v}(s)$ is known and $k(s|x)$ is the appropriate kernel for the unknown monopole or dipole source distribution as indicated in equation (7b) and (9b) respectively.

The unknown line source density distribution in equation (11) may be approximated by using any of several approximation methods, which leads to the generic representation

$$\sigma(x) = \sum_{i=1}^{N} h_i(x)\sigma_i, \tag{12}$$

where the h_i may be a set of orthogonal functions over the length of the line source, e.g., Legendre functions, or may be a suitable set of local basis or interpolation functions which are defined within a subinterval about x_i. As a limiting case of the latter class the h_i may be Dirac delta functions which result in a discrete approximation to the continuous distribution. It then follows from equations (11) and (12) that $\hat{v}(s)$ can be represented as

$$\hat{v}(s) = \sum_{i=1}^{N} K_i(s)\sigma_i, \tag{13a}$$

where the $K_i(s)$ are simply related to the kernel $k(s|x)$ as follows:

$$K_i(s) = \int k(s|x)h_i(x)\,\mathrm{d}x. \tag{13b}$$

For an $M > N$ point collocation on the surface S, it follows from equation (13) that

$$\hat{v}(s_m) = \sum_{i=1}^{N} K_i(s_m)\sigma_i, \qquad m = 1, \ldots, M, \tag{14a}$$

which can also be expressed in matrix form as

$$[\mathbf{K}]\boldsymbol{\sigma} = \mathbf{v}, \tag{14b}$$

where $[\mathbf{K}]$ is an $M \times N$ matrix with $M > N$. SVD methods [11] can then be used to express $\boldsymbol{\sigma}$ as

$$\boldsymbol{\sigma} = [\mathbf{K}]^{\dagger}\mathbf{v}, \tag{15}$$

where $[\mathbf{K}]^{\dagger}$ denotes the pseudo-inverse of $[\mathbf{K}]$. It is noted that, for the overdetermined system of interest here, in which $M > N$, SVD produces a solution that is the best approximation in the least squares sense: i.e., the solution vector is determined so as to minimize J_d, where

$$J_d = |[K]\boldsymbol{\sigma} - \mathbf{v}|^2. \tag{16}$$

Once the monopole and dipole source densities are determined from equation (15), the corresponding surface pressures can then be determined from equations (7a) and (9a) respectively by using simple quadrature methods. The resulting surface pressure could then be substituted into the Helmholtz integral solution for the external pressure field and the external pressure field could be simply determined by using quadrature methods as noted in earlier papers. In contrast to the use of the Helmholtz integral solution, the external pressure field can also be evaluated directly from equations (6a) and (8) by using simple quadrature methods. Although this latter approach is valid for both the near and far field it is particularly appealing for the far field, where Fourier transform methods can be introduced to provide additional insight into the general approach, as shown in the following section.

In order to obtain the desired Fourier transform relationships, it is first noted that for field points at large distances from the cylindrical surface of interest, the free space two-dimensional Green function of interest can be approximated as

$$[g(\mathbf{x}, \mathbf{x}_0)]_{y_0 = 0} \sim -(\mathrm{j}/4)\sqrt{2/\pi kR}\,\mathrm{e}^{-\mathrm{j}(kR - x_0 \cos\phi - \pi/4)}, \tag{17}$$

where (R, ϕ) denotes the cylindrical co-ordinates of the point of interest. It then follows that the kernel of equation (9b) can be approximated as follows:

$$\left.\frac{\partial g(\mathbf{x}, \mathbf{x}_0)}{\partial y_0}\right]_{y_0 = 0} \sim -\frac{k \sin\phi}{4}\sqrt{\frac{2}{\pi kR}}\,\mathrm{e}^{-\mathrm{j}(kR - x_0 \cos\phi - \pi/4)}. \tag{18}$$

The monopole and dipole far field pressures in equations (6a) and (8) can then be expressed as

$$p_m(R, \phi) \sim (k\rho_0 c_0/4)\sqrt{2/\pi kR}\,\mathrm{e}^{-\mathrm{j}(kR - \pi/4)}\bar{\sigma}_m(k \cos\phi) \tag{19a}$$

and

$$p_d(R, \phi) \sim (k/4)\sqrt{2/\pi kR}\, e^{-j(kR - \pi/4)} \bar{\sigma}_d(k \cos \phi) \sin \phi, \tag{19b}$$

where $\sigma_m(k_x)$ and $\sigma_d(k_x)$ are simply one-dimensional Fourier transforms of the corresponding source distributions; i.e.,

$$\bar{\sigma}_m(k_x) = \int_{-\infty}^{\infty} \sigma_m(x)\, e^{jk_x x}\, dx, \qquad \bar{\sigma}_d(k_x) = \int_{-\infty}^{\infty} \sigma_d(x)\, e^{jk_x x}\, dx. \tag{20a, b}$$

3. SPECIAL CASES

Several results of a general nature for the internal multi-pole source distributions introduced in the preceding section are first presented here for the case of cross-sectional areas S which exhibit reflective symmetry. By definition, such surfaces are symmetric about both the x- and y-axes, as illustrated in Figure 3. If the normal veolcity on the surface S is symmetric or antisymmetric about y, each of the multipole distributions exhibits the same symmetry as a function of x.

As an example of interest, consider a velocity distribution $v(s)$ which is an even function of s, i.e., $v(s) = v^e(s)$, and is also even about the y-axis. It is apparent from the preceding development that $\sigma_m(x) = \sigma_m(-x)$ is a symmetric function. For the case in which the velocity distribution $v(s)$ is an even function of s, i.e., $v(s) = v^e(s)$, and is odd about the y-axis, it is apparent that $\sigma_m(x) = -\sigma_m(-x)$ is an antisymmetric function. For this latter class of functions, the Fourier transform relationship (6a) can then be simply used to show that the pressure is zero on the y-axis. Similar arguments for velocity distributions which are odd functions of s, i.e., $v(s) = v^o(s)$, and also odd about the y-axis, results in antisymmetric dipole distributions for which $\sigma_d(x) = -\sigma_d(-x)$. For this latter class of functions, the pressure is zero on both the x- and y-axes.

Now consider the special case of a circular cylinder with a radius a, as indicated in Figure 4. The acoustic radiation and scattering from such a cylinder is a classical boundary value problem which is readily solved by using the method of separation of variables [12] to address the problem as stated in equations (1) and (2). Since closed form solutions for these problems can be readily obtained, such solutions can be used to obtain insight into the nature of the source distributions which form the basis of the internal source density method presented here to solve the problems.

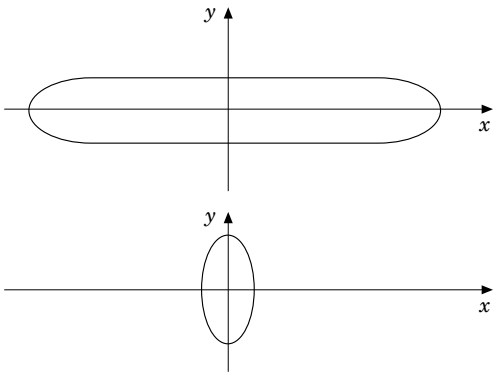

Figure 3. Examples of reflective surfaces.

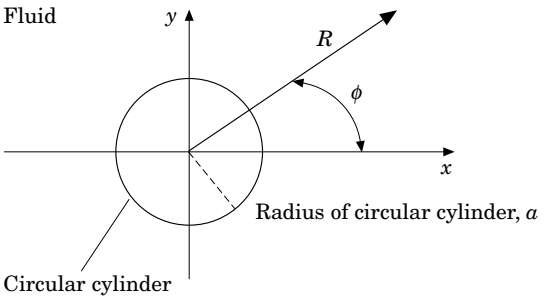

Figure 4. A circular cylinder.

In general, the normal velocity distribution of interest on the surface can be expressed as the Fourier series

$$v(a, s) = \sum_{n=0}^{\infty} V_n \cos(ns/a) + \sum_{n=1}^{\infty} U_n \sin(ns/a), \tag{21a}$$

where $s = a\phi$. The associated pressure field in the fluid can similarly be expressed as a Fourier series in which the coefficients are simply obtained by matching the normal velocity at the boundary to obtain the following expansion:

$$p(R, \phi) = -\mathrm{j}\rho_0 c_0 \sum_{n=0}^{\infty} \frac{\mathrm{H}_n(kR)}{\mathrm{H}_n'(ka)} [V_n \cos(n\phi) + U_n \sin(n\phi). \tag{21b}$$

In order to obtain an insight into the nature of the internal source distributions for such a problem, it is sufficient to consider only a single circumferential harmonic, i.e.,

$$v(a, \phi) = V_n \cos(n\phi) + U_n \sin(n\phi), \tag{22}$$

where n is now an arbitrary positive integer. It is obvious that the $\cos(n\phi)$ is associated with a linear monopole distribution $\sigma_{m,n}(x)$, whereas the $\sin(n\phi)$ is associated with a linear dipole distribution $\sigma_{d,n}(x)$. If the internal source distributions for such a problem can be determined, superposition can simply be used to address the more general acoustic radiation and scattering problem of interest.

It is apparent from equation (21b) that the external pressure field corresponding to the velocity in equation (22) can be expressed as

$$p(R, \phi) = -\mathrm{j}\rho_0 c_0 \frac{\mathrm{H}_n(kR)}{\mathrm{H}_n'(ka)} [V_n \cos(n\phi) + U_n \sin(n\phi)]. \tag{23a}$$

After using the asymptotic form of the Hankel function for $kR \gg n$ in equation (23a) it is readily apparent that the associated far field pressure for the circumferential mode can be expressed as

$$p(R, \phi) = \sqrt{\frac{2}{\pi kR}}\, \mathrm{e}^{-\mathrm{j}(kR - \pi/4)} \frac{-\mathrm{j}\rho_0 c_0\, \mathrm{e}^{-\mathrm{j}n\pi/4}}{\mathrm{H}_n'(ka)} [V_n \cos(n\phi) + U_n \sin(n\phi)]. \tag{23b}$$

Upon recalling that the far field presssure has been expressed as a function of the internal source distributions in equation (19), the following Fourier transforms or integral

TABLE 1

c_{ni} coefficients versus n and i

n	$i=0$	$i=1$	$i=2$	$i=3$
0	1	0	0	0
1	0	1	0	0
2	−1	0	2	0
3	0	−3	0	4

equations of the first kind are obtained for the internal source distributions by equating the results in equations (19) and (20) to the corresponding components in equation (23):

$$\int_{-\infty}^{\infty} \sigma_{m,n}(x)\, \mathrm{e}^{\mathrm{j}k\cos(\phi)x}\, \mathrm{d}x = -\mathrm{j}^{n+1} \frac{4V_n}{k\mathrm{H}_n'(ka)} \cos(n\phi) \tag{24a}$$

and

$$\sin(\phi) \int_{-\infty}^{\infty} \sigma_{d,n}(x)\, \mathrm{e}^{\mathrm{j}k\cos(\phi)x}\, \mathrm{d}x = \mathrm{j}^{n+1} \frac{4\rho_0 c_0 U_n}{k\mathrm{H}_n'(ka)} \sin(n\phi). \tag{24b}$$

In order to determine $\sigma_{m,n}(x)$ and $\sigma_{d,n}(x)$ by using equation (24), de Moivre's identity is first noted:

$$\mathrm{e}^{\mathrm{j}n\phi} = [\cos(\phi) + \mathrm{j}\sin(\phi)]^n. \tag{25}$$

After equating the real and imaginary parts of both sides of the equation, it is apparent that

$$\cos(n\phi) = \sum_{i=0}^{n} c_{ni} \cos^i(\phi) \tag{26a}$$

and

$$\sin(n\phi) = \sin(\phi) \sum_{i=0}^{n} s_{ni} \cos^i(\phi), \tag{26b}$$

where the c_{ni} and s_{ni} are constants [13]. It is noted for n even (odd) that $c_{ni} = 0$ for i odd (even). For n even (odd) it is noted that $s_{ni} = 0$ for i even (odd). Tabulated values of c_{ni} and s_{ni} are presented in Tables 1 and 2 for $n = 0$, 1, 2 and 3.

TABLE 2

s_{ni} coefficients versus n and i

n	$i=0$	$i=1$	$i=2$	$i=3$
0	0	0	0	0
1	1	0	0	0
2	−0	2	0	0
3	−1	0	4	0

Now $\sigma_{m,n}(x)$ can be determined via the substitution of equation (26a) into equation (24a), to obtain

$$\int_{-\infty}^{\infty} \sigma_{m,n}(x)\, \mathrm{e}^{\mathrm{j}k\cos(\phi)x}\, \mathrm{d}x = -\mathrm{j}^{n+1} \frac{4V_n}{k\mathrm{H}_n'(ka)} \sum_{i=0}^{n} c_{ni} \cos^i(\phi). \tag{27}$$

After noting the following property of the Dirac delta function $\delta(x)$,

$$\int_{-\infty}^{\infty} \delta^{(p)}(x)\, \mathrm{e}^{\mathrm{j}k\cos(\phi)x}\, \mathrm{d}x = (-\mathrm{j}k\cos(\phi))^p, \tag{28}$$

where $\delta^{(p)}(x)$ denotes the pth derivative, it then follows that

$$\sigma_{m,n}(x) = -\mathrm{j}^{n+1} \frac{4V_n}{k\mathrm{H}_n'(ka)} \sum_{i=0}^{n} c_{ni} \frac{\delta^{(i)}(x)}{(-\mathrm{j}k)^i}. \tag{29a}$$

A similar expression for $\sigma_{d,n}(x)$ is also readily obtained via the same procedure: i.e.,

$$\sigma_{d,n}(x) = \mathrm{j}^{n+1} \frac{4\rho_0 c_0 U_n}{k\mathrm{H}_n'(ka)} \sum_{i=0}^{n} s_{ni} \frac{\delta^{(i)}(x)}{(-\mathrm{j}k)^i}. \tag{29b}$$

Expressions for the external pressure fields for the internal line source distributions in equations (29) are presented in the Appendix.

In the light of the exact solution for the internal source distributions in equation (29), several observations regarding the use of the ISD/SVD method for circular cylinders are readily apparent. Since $\delta^{(i)}(x)$ is an even (odd) generalized function for i even (odd), and for n even (odd) it was noted that $c_{ni} = 0$ for i odd (even), then $\sigma_{m,n}(x)$ is an even (odd) function for n even (odd). It then follows from earlier discussion that the pressure is zero on the y-axis for n odd. This is of course an expected result, since the associated field is proportional to $\cos n\phi$. Via the same type of argument it is apparent that $\sigma_{d,n}(x)$ is an odd (even) function for n odd (even). It then follows from earlier discussion that the pressure is zero on the y-axis for n even since the associate field is proportional to $\sin(n\phi)$.

Most striking about the exact solution for the internal source distributions in equations (29), however, is the singular behaviour and the limited region of support of the source distribution about the origin due to the nature of the Dirac delta function and its derivatives. Clearly, as n increases the region of support for any discrete numerical approximation of $\sigma_{m,n}(x)$ will increase, the peak amplitudes will increase and the resultant approximation will become more oscillatory. These results are most simply obtained via the use of central difference approximations to the derivatives of the Dirac delta functions. Also, as ka increases the maximum number of n for a specified problem will also generally increase. It is thus to be expected that high frequency problems will be more formidable to address by using the ISD/SVD method. In contrast to the use of the normal equations to solve the least mean square error problem for small ka, the present analysis indicates that SVD methods would be required for large ka. These conclusions are consistent with the observations noted during recent numerical studies conducted with the method [8–10].

In order to provide some insight into the characteristics of the internal source density distributions for cylinders with large aspect ratios, the geometry shown in Figure 5 is now addressed. In contrast to the circular cylinder with an aspect ratio of unity, the aspect ratio for the indicated configuration is $L/a + 1$. Rather than address the case in which L/a is finite, the limiting case of L/a infinite is addressed here. Although edge effects are not

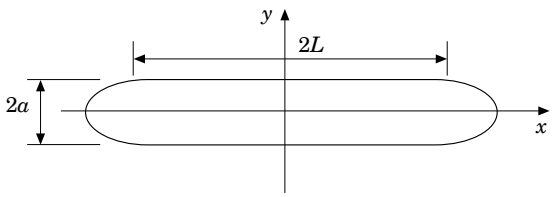

Figure 5. A rectangular cylinder with hemi-cylindrical endcaps.

present in the following analysis, the analysis provides additional insight into the use of the ISD/SVD method for cylinders with large aspect ratios.

Now consider the limiting case of the geometry shown in Figure 5, where the normal velocity over the planar surfaces $y = \pm a$ is symmetric about the mid-surface: i.e., $v(x, a) = -v(x, -a)$. The normal velocity is denoted as

$$v(s, a) = V_0 \cos(\beta s), \tag{30}$$

where s is now measured from the origin $x = 0$ and β is a constant. Since the normal velocity is symmetric about the mid-surface plane $y = 0$, the internal source distribution of interest is clearly a linear monopole source distribution denoted here as $\sigma_m(x)$.

It is apparent from equation (7b) that $\sigma_m(x)$ must satisfy the following integral equation of the first kind:

$$V_0 \cos(\beta s) = \int_{-\infty}^{\infty} -\hat{\mathbf{n}} \cdot \nabla_s [g(\mathbf{x}_s, \mathbf{x}_0)]_{y_0 = 0} \sigma_m(x_0)\, \mathrm{d}x_0, \qquad y_s = a. \tag{31}$$

As a result of the periodicity of the normal velocity distribution in x, the internal monopole source distribution is represented as

$$\sigma_m(x) = \sigma_0 \cos(\beta x), \tag{32}$$

where σ_0 is to be determined. It then follows from equations (31) and (32) that

$$V_0 = -\sigma_0 \partial I / \partial y, \qquad y = a, \tag{33a}$$

where, due to the symmetric nature of the integrand, I is expressed as

$$I = \frac{-\mathrm{j}}{2} \int_0^{\infty} \mathrm{H}_0(k\sqrt{y^2 + x^2}) \cos(\beta x)\, \mathrm{d}x. \tag{33b}$$

The key to evaluating σ_0 is the following pair of integral identities [13]:

$$\int_0^{\infty} \mathrm{J}_0(\alpha\sqrt{y^2 + x^2}) \cos(\beta x)\, \mathrm{d}x = \left\{ \begin{array}{ll} \dfrac{\cos(y\sqrt{\alpha^2 - \beta^2})}{\sqrt{\alpha^2 - \beta^2}}, & 0 < \beta < \alpha,\ y > 0 \\ 0, & 0 < \alpha < \beta,\ y > 0 \end{array} \right\} \tag{34a}$$

and

$$\int_0^{\infty} \mathrm{Y}_0(\alpha\sqrt{y^2 + x^2}) \cos(\beta x)\, \mathrm{d}x = \left\{ \begin{array}{ll} \dfrac{\sin(y\sqrt{\alpha^2 - \beta^2})}{\sqrt{\alpha^2 - \beta^2}}, & 0 < \beta < \alpha,\ y > 0 \\ -\dfrac{\mathrm{e}^{-y\sqrt{\beta^2 - \alpha^2}}}{\sqrt{\beta^2 - \alpha^2}}, & 0 < \alpha < \beta,\ y > 0 \end{array} \right\}. \tag{34b}$$

It then follows for $\alpha = k$ and $\beta > 0$ that I can be expressed as

$$I = \left\{ \begin{array}{ll} -\frac{\mathrm{j}}{2} \dfrac{\mathrm{e}^{-\mathrm{j}y\sqrt{k^2-\beta^2}}}{\sqrt{k^2-\beta^2}}, & 0 < \beta < k \\ \frac{1}{2} \dfrac{\mathrm{e}^{-y\sqrt{\beta^2-k^2}}}{\sqrt{\beta^2-k^2}}, & 0 < k < \beta \end{array} \right\}. \tag{35}$$

Finally, from equations (33a) and (35) it is apparent that σ_0 may be expressed as

$$\sigma_0 = \left\{ \begin{array}{ll} 2V_0\, \mathrm{e}^{\mathrm{j}a\sqrt{k^2-\beta^2}}, & 0 < \beta < k \\ 2V_0\, \mathrm{e}^{a\sqrt{\beta^2-k^2}}, & 0 < k < \beta \end{array} \right\}. \tag{36}$$

As a check on the above result, it is noted that if $\sigma_m(x)$ is substituted into equation (6a) and the resultant integral evaluated for $y > a$ by using the integrals in equations (34), the following expression is obtained for the pressure field:

$$p(\mathbf{x}) = \left\{ \begin{array}{ll} \dfrac{k\rho_0 c_0 V_0}{\sqrt{k^2-\beta^2}} \cos(\beta x)\, \mathrm{e}^{-\mathrm{j}(y-a)\sqrt{k^2-\beta^2}}, & 0 < \beta < k \\ \dfrac{\mathrm{j}k\rho_0 c_0 V_0}{\sqrt{\beta^2-k^2}} \cos(\beta x)\, \mathrm{e}^{-(y-a)\sqrt{\beta^2-k^2}}, & 0 < k < \beta \end{array} \right\}. \tag{37}$$

The expression (37) clearly satisfies the boundary conditions and the Helmholtz equation and is thus the solution to the boundary value problem of interest. Of course, for this problem the solution is obtained more directly via the method of separation of variables.

The solution for $\sigma_m(x)$ defined in equations (32) and (36) is noted to exhibit significantly different characteristics from the monopole source density distribution for the circular cylinder. In contrast to the circular cylinder, the region of support is not confined to the origin but is in fact the entire plane of symmetry. In addition, the spatial dependence of the source density for the "large aspect cylinder" matches the spatial variation of the normal velocity on the surface which is in contrast to that of the circular cylinder.

It is now noted that β is a free parameter in the solution for the "large aspect cylinder". If V_0 is considered now to be an even function of β, more general spatially bounded normal velocity distributions which are symmetric functions of x (and thus s) may be represented via an integration over β, i.e.,

$$v(s, a) = \frac{1}{2\pi} \int_{-\infty}^{\infty} V_0(\beta) \cos(\beta s)\, \mathrm{d}\beta \tag{38a}$$

or, equivalently,

$$v(s, a) = \frac{1}{2\pi} \int_{-\infty}^{\infty} V_0(\beta)\, \mathrm{e}^{-\mathrm{j}\beta s}\, \mathrm{d}\beta. \tag{38b}$$

It is then apparent that $V_0(\beta)$ is the Fourier transform of the spatially bounded normal symmetric velocity distributions $v(s, a)$: i.e.,

$$V_0(\beta) = \int_{-\infty}^{\infty} v(s, a)\, \mathrm{e}^{\mathrm{j}\beta s}\, \mathrm{d}s. \tag{39}$$

The associated $\sigma_m(x)$ for the spatially bounded normal velocity distributions can also be obtained by integration over β:

$$\sigma_m(x) = \frac{1}{2\pi} \int_{-\infty}^{\infty} 2V_0(\beta)\, \mathrm{e}^{-\mathrm{j}a\sqrt{k^2-\beta^2}}\, \mathrm{e}^{-\mathrm{j}\beta x}\, \mathrm{d}x. \tag{40}$$

Similarly, after performing an integration over β in equation (37) the following expression for the associated pressure is obtained for $y > a$:

$$p(\mathbf{x}) = \frac{1}{2\pi} \int_{-\infty}^{\infty} \frac{k\rho_0 c_0 V_0(\beta)}{\sqrt{k^2-\beta^2}} \cos(\beta x)\, \mathrm{e}^{-\mathrm{j}(y-a)\sqrt{k^2-\beta^2}}\, \mathrm{d}\beta, \tag{41a}$$

or, equivalently,

$$p(\mathbf{x}) = \frac{1}{2\pi} \int_{-\infty}^{\infty} \frac{k\rho_0 c_0 V_0(\beta)}{\sqrt{k^2-\beta^2}}\, \mathrm{e}^{-\mathrm{j}(y-a)\sqrt{k^2-\beta^2}}\, \mathrm{e}^{-\mathrm{j}\beta x}\, \mathrm{d}\beta. \tag{41b}$$

Finally, the case of a spatially bounded normal velocity distribution on a rectangular cylinder of finite length as shown in Figure 5 is simply addressed from the preceding results for the limiting case of $a = 0$. It is apparent from equations (38) and (40) that $\sigma_m(x)$ for the spatially bounded normal velocity distributions can be expressed as

$$\sigma_m(x) = 2v(x, 0+). \tag{42}$$

The spatial regions of support for the normal velocity and the source density are thus identical. A direct application of the convolution property of Fourier transforms to equation (41b) then leads to

$$p(\mathbf{x}) = \mathrm{j}k\rho_0 c_0 \int 2[g(\mathbf{x}, \mathbf{x}_0)]_{y_0=0} v(x_0, 0)\, \mathrm{d}x_0, \tag{43}$$

which is in agreement with the well known Rayleigh integral solution for the planar problem [12]. These latter results are of course to be expected for the limiting case.

4. SUMMARY AND CONCLUSIONS

Two-dimensional harmonic radiation and scattering problems arise in many areas of mathematical physics. Although the focus in the present paper is on acoustic two-dimensional harmonic radiation and rigid body scattering problems from cylinders of arbitrary shape with a plane of symmetry, the approach and results are obviously applicable to a wide range of physical problems which are described mathematically by the reduced wave equation and Neumann boundary conditions.

A previously developed LMS error method [8–10] has been used to solve the Neumann boundary value problem via the use of an internal line monopole and dipole source distribution along the plane of symmetry. SVD methods were presented to determine the line source harmonic multipole distributions from the specified normal velocity at the cylindrical surface. Field pressures were simply obtained from line integrals of the source distributions which, in the far field, reduce to Fourier transform relationships.

Exact expressions for the source strength distributions corresponding to acoustic two-dimensional harmonic radiation and rigid body scattering from circular cylinders were developed by using asymptotic and Fourier transform relationships. The resulting source

strength distributions involve spatial derivatives of Dirac delta functions and thus have a vanishingly small region of support about the center of the cylinder. The spatial characteristics of the distributions indicate that problems involving circular cylinders provide formidable test problems for the general approach. Earlier numerical studies [8–10] indicated typical accuracy and the suitability of the method for addressing such problems.

In order to provide an insight into the nature of the line source distributions for cylinders with large aspect ratios, the spatial characteristics of the source strength distributions were investigated for the geometry of a thin rectangular cylinder with hemi-cylindrical endcaps. In general, the spatial characteristics of the source strength distributions are closely matched to the normal velocity distribution for large aspect configurations. For the limiting case of an infinitesimally thin rectangular cylinder with a symmetric velocity distribution about the plane of symmetry, the combined internal source distribution (ISD/SVD) method provides an alternative development of the well known classical Rayleigh solution to the planar Neumann boundary value problem.

In conclusion, several additional points of interest regarding the use of the combined ISD/SVD method to address acoustic two-dimensional harmonic radiation and scattering from cylinders with a plane of symmetry are noted. First, it is noted the line source distributions are restricted to the region within the cylinder on the plane of symmetry and are thus not in the external fluid region of interest. The resulting field within the internal region is non-physical and of no significance to the exterior problem. In this regard the source distributions here are introduced in a manner closely related to the well known introduction of image sources to address scattering from an ideally pressure release or rigid planar boundary [14].

As a second point, it is noted that although the ISD/SVD method has been applied here to problems involving separable geometries for which closed form solutions exist, the basic method is applicable to address acoustic radiation and scattering problems from rigid or elastic bodies with a plane of symmetry. The applicability of the basic method to the general acoustic radiation and rigid body scattering problem has already been previously noted [8, 9]. Since the ISD/SVD method can be used to evaluate modal acoustic radiation impedances [10], the more general acoustic radiation and scattering problem from an elastic cylinder is readily addressed using the *in vacuo* eigenvectors of the structure as the basis functions for the fluid loaded problem. The general procedure to address the two-dimensional radiation and scattering problem from elastic cylinders is noted to be analogous to that presented for the axisymmetric radiation and scattering from elastic shells of revolution [15].

Finally, it is noted that there is an inherent restriction on the method which is associated with the smoothness of the cylindrical surface S. It is well known that the field or the gradient of the field in the vicinity of the vertex of a wedge can exhibit a singular behaviour [1–3]. Since the external field from any internal line source distribution is free of such singularities it is obvious that the combined ISD/SVD method is not applicable to cylindrical shapes in which there is not a unique tangent plane at each point on the contour.

REFERENCES

1. P. M. Morse and H. Feshbach 1953 *Methods of Theoretical Physics*. New York: McGraw-Hill.
2. I. Stakgold 1967 *Boundary Value Problems in Mathematical Physics*. New York: Macmillan.
3. D. G. Crighton, A. P. Dowling, J. E. Ffowcs Williams, M. Heckl and F. G. Leppington 1992 *Modern Methods in Analytical Acoustics—Lecture Notes*. London: Springer-Verlag.
4. J. J. Bowman, T. B. A. Senior and P. L. E. Uslenghi 1969 *Electromagnetic and Acoustic Scattering by Simple Shapes*. Amsterdam: North-Holland.

5. L. H. CHEN and D. G. SCHWEIKERT 1963 *Journal of the Acoustical Society of America* **35**, 1626–1632. Sound radiation from an arbitrary body.
6. H. A. SCHENCK 1967 *Journal of the Acoustical Society of America* **44**, 41–48. Improved integral formulation for acoustic radiation problems.
7. A. J. BURTON and G. F. MILLER 1971 *Proceedings of the Royal Society*, *London A* **323**, 201–210. The application of integral equation methods to the numerical solution of some exterior boundary-value problems.
8. P. R. STEPANISHEN and S. RAMAKRISHNA 1993 *Journal of the acoustical Society of America* **93**, 658–672. Acoustic radiation from cylinders with a plane of symmetry using internal multipole source distributions, I.
9. S. RAMAKRISHNA and P. R. STEPANISHEN 1993 *Journal of the Acoustical Society of America* **93**, 673–682. Acoustic scattering from cylinders with a plane of symmetry using internal multipole source distributions, II.
10. P. R. STEPANISHEN and S. RAMAKRISHNA 1994 *Journal of Sound and Vibration*. **176**, 49–68. Acoustic impedances and impulse responses for elliptical cylinders using internal source density and SVD methods.
11. W. H. PRESS, B. P. FLANNERY, S. A. TEUKOLSKY and W. T. VETTERLING 1986 *Numerical Recipes*, Cambridge: Cambridge University Press.
12. M. C. JUNGER and D. FEIT 1972 *Sound*, *Structures and their interaction*, Cambridge, MA: MIT Press.
13. I. GRADSHTEYN and I. M. RYZHIK 1980 *Tables of Integrals*, *Series and Products*, editor A. Jeffreys. London: Academic Press.
14. P. M. MORSE and K. U. INGARD 1968 *Theoretical Acoustics*. New York: McGraw-Hill.
15. P. R. STEPANISHEN and H. W. CHEN 1992 *Journal of the Acoustical Society of America* **92**, 2248–2259. Acoustic radiation and scattering from shells of revolution using finite element and internal source density methods.

APPENDIX: THE EXTERNAL PRESSURE FIELD FROM A CIRCULAR CYLINDER

Consider the circular cylinder shown in Figure 4, with a normal velocity which corresponds to a single circumferential harmonic, i.e.,

$$v(a, \phi) = V_n \cos(n\phi) + U_n \sin(n\phi), \tag{A1}$$

where n is an arbitrary positive integer. The associated external pressure field can be expressed as

$$p(\mathbf{x}) = p^e(\mathbf{x}) + p^a(\mathbf{x}), \qquad |\mathbf{x}| > a, \tag{A2}$$

where

$$p^e(\mathbf{x}) = p_{m,n}(\mathbf{x}) = \mathrm{j}k\rho_0 c_0 \int [g(\mathbf{x}, \mathbf{x}_0)]_{y_0 = 0} \sigma_{m,n}(x_0)\, \mathrm{d}x_0 \tag{A3a}$$

and

$$p^0(\mathbf{x}) = p_{d,n}(\mathbf{x}) = \int \left[\frac{\partial g(\mathbf{x}, \mathbf{x}_0)}{\partial y_0}\right]_{y_n = 0} \sigma_{d,n}(x_0)\, \mathrm{d}x_0 \tag{A3b}$$

and where $\sigma_{m,n}(x)$ and $\sigma_{d,n}(x)$ are defined in equations (29).

After noting the following property of the Dirac delta function $\delta(x)$,

$$\int_{-\infty}^{\infty} \delta^{(p)}(x)\gamma(x)\, \mathrm{d}x = (-1)^p \gamma^{(p)}(0), \tag{A4}$$

it is easily shown that

$$p_{m,n}(\mathbf{x}) = \mathrm{j}^n \frac{4\rho_0 c_0 V_n}{\mathrm{H}_n'(ka)} \sum_{i=0}^{n} \frac{c_{ni}}{(jk)^i} \left[\frac{\partial^i g(\mathbf{x}, \mathbf{x}_0)}{\partial x_0^i} \right]_{\mathbf{x}_0 = 0} \tag{A5a}$$

and

$$p_{d,n}(\mathbf{x}) = \mathrm{j}^{n+1} \frac{4\rho_0 c_0 V_n}{k\mathrm{H}_n'(ka)} \sum_{i=0}^{n} \frac{s_{ni}}{(jk)^i} \left[\frac{\partial^i G(\mathbf{x}, \mathbf{x}_0)}{\partial x_0^i} \right], \tag{A5b}$$

where

$$g(\mathbf{x}, \mathbf{x}_0) = -\mathrm{j}/4\, \mathrm{H}_0(k\sqrt{(x-x_0)^2 + (y-y_0)^2}) \qquad \text{and} \qquad G(\mathbf{x}, \mathbf{x}_0) = \lim_{y_0 - 0} \frac{\partial g(\mathbf{x}, \mathbf{x}_0)}{\partial y_0}. \tag{A6a,b}$$

After performing the operation in equation (A6b), it is easily shown that

$$G(\mathbf{x}, \mathbf{x}_0) = -\frac{\mathrm{j}y}{4\sqrt{(x-x_0)^2 + (y-y_0)^2}} \mathrm{H}_1(k\sqrt{(x-x_0)^2 + (y-y_0)^2}). \tag{A6c}$$

It is noted that equation (A5) provides an alternative description of the pressure field to the expression in equation (23a). It is then apparent from equations (A3) and (A5) that the series in equation (A5a), [A5b] must be equivalent to the first (second) term in equation (23a). Rather than address the general case, several specific cases are addressed in the following paragraphs to illustrate the equivalence.

First, consider, the case of $n = 0$ in equation (A5a), which leads to

$$p_{m,0}(\mathbf{x}) = \frac{4\rho_0 c_0 V_n}{\mathrm{H}_0'(ka)} c_{00}[g(\mathbf{x}, \mathbf{x}_0)]_{\mathbf{x}_0 = 0}. \tag{A7}$$

Equation (A7) can be expressed by using the coefficients in Table 1 as

$$p_{m,0}(\mathbf{x}) = -\mathrm{j}\rho_0 c_0 \frac{\mathrm{H}_0(kR)}{\mathrm{H}_0'(ka)} V_0, \tag{A8}$$

which is in agreement with the analogous result from equation (23a). The case of $n = 1$ in equation (A5a) is also simply addressed and leads to

$$p_{m,1}(\mathbf{x}) = \mathrm{j} \frac{4\rho_0 c_0 V_1}{\mathrm{H}_1'(ka)} \frac{1}{(jk)} \left[\frac{\partial g(\mathbf{x}, \mathbf{x}_0)}{\partial x_0} \right]_{\mathbf{x}_0 = 0}. \tag{A9}$$

Since

$$[\partial g(\mathbf{x}, \mathbf{x}_0)/\partial x_0]_{\mathbf{x}_0 - 0} = \mathrm{j} \cos(\phi) k \mathrm{H}_0'(kR), \tag{A10}$$

it then follows that

$$p_{m,1}(\mathbf{x}) = \mathrm{j}\rho_0 c_0 \frac{\mathrm{H}_i(kR)}{\mathrm{H}_1'(ka)} V_1 \cos(\phi), \tag{A11}$$

which is in agreement with the analogous result from equation (23a). Finally the case of $n = 2$ in Equation (A5a) is also simply addressed and leads to

$$p_{m,2}(\mathbf{x}) = \frac{4\rho_0 c_0 V_2}{\mathrm{H}_2'(ka)}\left[g(\mathbf{x}, \mathbf{x}_0) + \frac{2}{k^2}\left[\frac{\partial^2 g(\mathbf{x}, \mathbf{x}_0)}{\partial x_0^2}\right]_{\mathbf{x}_0 - 0}\right] \tag{A12}$$

where

$$\left[\frac{\partial^2 g(\mathbf{x}, \mathbf{x}_0)}{\partial x_0^2}\right]_{\mathbf{x}_0 = 0} = -\frac{\mathrm{j}k}{4R}\left[\sin^2(\phi)\mathrm{H}_0'(kR) + \cos^2(\phi)\mathrm{H}_0'(kR)kR\right]. \tag{A13}$$

After noting that

$$kR\mathrm{H}_0''(kR) = -kR\frac{\mathrm{dH}_1(kR)}{\mathrm{d}(kR)}, \tag{A14a}$$

and

$$kR\frac{\mathrm{dH}_1(kR)}{\mathrm{d}(kR)} = kR\mathrm{H}_0(kR) - \mathrm{H}_1(kR), \tag{A14b}$$

simple algebraic manipulations lead to the expression

$$p_{m,2}(\mathbf{x}) = -\mathrm{j}\rho_0 c_0 \frac{\mathrm{H}_2(kR)}{\mathrm{H}_2'(ka)} V_2 \cos(2\phi), \tag{A15}$$

which is of course the expected result from equation (23a).